A model for the diffuse attenuation coefficient of downwelling irradiance

Zhong-Ping Lee[1]
Naval Research Laboratory, Stennis Space Center, Mississippi, USA

Ke-Ping Du
State Key Laboratory of Remote Sensing Science, Research Center for Remote Sensing and GIS, School of Geography, Beijing Normal University, Beijing, China

Robert Arnone
Naval Research Laboratory, Stennis Space Center, Mississippi, USA

Received 9 January 2004; revised 13 August 2004; accepted 28 December 2004; published 22 February 2005.

[1] The diffuse attenuation coefficient for downwelling irradiance (K_d) is an important parameter for ocean studies. For the vast ocean the only feasible means to get fine-scale measurements of K_d is by ocean color remote sensing. At present, values of K_d from remote sensing are estimated using empirical algorithms. Such an approach is insufficient to provide an understanding regarding the variation of K_d and contains large uncertainties in the derived values. In this study a semianalytical model for K_d is developed based on the radiative transfer equation, with values of the model parameters derived from Hydrolight simulations using the averaged particle phase function. The model is further tested with data simulated using significantly different particle phase functions, and the modeled K_d are found matching Hydrolight K_d very well (~2% average error and ~12% maximum error). Such a model provides an improved interpretation about the variation of K_d and a basis to more accurately determine K_d (especially using data from remote sensing).

Citation: Lee, Z.-P., K.-P. Du, and R. Arnone (2005), A model for the diffuse attenuation coefficient of downwelling irradiance, *J. Geophys. Res.*, *110*, C02016, doi:10.1029/2004JC002275.

1. Introduction

[2] Diffuse attenuation coefficient for downwelling irradiance (K_d) (see Table 1 for symbols and definitions used in this text) is an important property for ocean studies. K_d can be used to classify water classes [*Jerlov*, 1976], and K_d is a critical parameter for accurate estimation of the light intensity at depth [*Simpson and Dickey*, 1981]. For the vast ocean, satellite remote sensing is the only feasible means to get repetitive and fine-scale measurements of K_d. At present, the standard method to estimate values of K_d from remotely sensed data is through empirical relationships between K_d and the spectral ratio of water-leaving radiance at two wavelengths [*Austin and Petzold*, 1981; *Mueller and Trees*, 1997]. Such an approach is insufficient to provide an understanding regarding the variation of K_d and, contains large uncertainties inherent to empirical algorithms [*Mueller*, 2000]. For the estimation of K_d, which is important for studies of heat budgets [*Lewis et al.*, 1990; *Morel and Antoine*, 1994; *Ohlmann et al.*, 1996; *Zaneveld et al.*, 1981] and photosynthesis [*Marra et al.*, 1995; *Platt et al.*, 1988; *Sathyendranath et al.*, 1989], a model that can provide better accuracy is desired. In this study, after a brief review of historical descriptions regarding K_d, we developed a semianalytical model based on the radiative transfer equation with model parameters evaluated from Hydrolight numerical simulations. Combined with existing semianalytical algorithms for the derivation of water's absorption and backscattering coefficients, this K_d model can then be easily implemented to semianalytically calculate values of K_d from remotely sensed data.

2. Background

[3] In ocean optics, spectral K_d at a geometric depth (so-called local value) is defined as [*Gordon et al.*, 1980]

$$K_d(z) = -\frac{1}{E_d(z)}\frac{dE_d(z)}{dz}, \tag{1}$$

with $E_d(z)$ the spectral downwelling irradiance at depth z and z pointing downward from the surface. Wavelength dependence is omitted for brevity. $K_d(z)$ is an apparent optical property (AOP) [*Preisendorfer*, 1976], which varies with the angular distribution of the light field [*Gordon*,

[1]Also visiting professor at Institute of Ocean Remote Sensing, Ocean University of China, Qingdao, China.

0148-0227/05/2004JC002275$09.00

Table 1. Symbols and Definitions[a]

Symbol	Definition	Units
a	absorption coefficient	m^{-1}
b	scattering coefficient	m^{-1}
b_b	backscattering coefficient	m^{-1}
$E_d(z)$ ($E_u(z)$)	downwelling (upwelling) irradiance at depth z	W m^{-2} nm^{-1}
$E_O(z)$	scalar irradiance at depth z	W m^{-2} nm^{-1}
$R(z)$	irradiance reflectance at depth z (= $E_u(z)/E_d(z)$)	
R_{rs}	remote sensing reflectance (ratio of water-leaving radiance to downwelling irradiance above the surface)	sr^{-1}
K_d	diffuse attenuation coefficient for downwelling irradiance	m^{-1}
$K_d(z)$	diffuse attenuation coefficient for downwelling irradiance at depth z, the so-called local value	m^{-1}
$\langle K_d \rangle$	K_d of the euphotic zone (between $E_d(0)$ and 1% of $E_d(0)$)	m^{-1}
$\overline{K}_d(z)$	diffuse attenuation coefficient for downwelling irradiance between 0 m and depth z	m^{-1}
$\overline{K}_d(E_{10\%})$	diffuse attenuation coefficient for downwelling irradiance between $E_d(0)$ and 10% of $E_d(0)$	m^{-1}
$\mu_d(z)$ ($\mu_u(z)$)	average cosine of downwelling (upwelling) light at depth z	
θ_a	above surface solar zenith angle	deg
μ_0	average cosine of subsurface downwelling light	

[a]Note that except θ_0, all other properties more or less vary with wavelength.

1989; *Gordon et al.*, 1975; *Kirk*, 1984]. Since the light distribution changes with depth [*Tyler*, 1960], $K_d(z)$ varies with z even for vertically homogenous waters before reaching an asymptotic value at greater depths [*Berwald et al.*, 1995; *Liu et al.*, 2002; *McCormick*, 1995; *McCormick and Hojerslev*, 1994; *Zaneveld*, 1989].

[4] To know the vertical variation of $K_d(z)$, $E_d(z)$ needs to be measured within a infinitesimal range of z (see equation (1)). In the field measurements of K_d, wave-introduced fluctuations in the subsurface light field make it nearly impossible to accurately determine $K_d(z)$. To overcome this obstacle, a common and useful practice is to calculate the diffuse attenuation coefficient between the irradiances measured over distant depths and get

$$\overline{K}_d(z_1 \leftrightarrow z_2) = \frac{1}{z_2 - z_1} \ln\left(\frac{E_d(z_1)}{E_d(z_2)}\right), \tag{2}$$

with z_1 and z_2 far apart to ensure reliable measurements of E_d change. In addition, when there are vertical profiles of $E_d(z)$, $\overline{K}_d(z_1 \leftrightarrow z_2)$ is usually derived by linear regression analysis between $\ln(E_d(z))$ and z [*Darecki and Stramski*, 2004; *Smith and Baker*, 1981]. Clearly, this $\overline{K}_d(z_1 \leftrightarrow z_2)$ or $\overline{K}_d$ is not exactly the $K_d(z)$ defined by equation (1). However, this $\overline{K}_d(z_1 \leftrightarrow z_2)$ is more useful than $K_d(z)$ [*McCormick and Hojerslev*, 1994] since known $\overline{K}_d(z_1 \leftrightarrow z_2)$ and $E_d(z_1)$ (or $E_d(z_2)$) makes it easy to calculate $E_d(z_2)$ (or $E_d(z_1)$). For estimating the light intensity at a depth z [*Sathyendranath and Platt*, 1988], it is $\overline{K}_d(z)(\equiv \overline{K}_d(0 \leftrightarrow z)$, the averaged attenuation coefficient between surface and z) needed, not the local value $K_d(z)$. Also, for measurements made by sensors at fixed depths (e.g., MOBY [*Clark et al.*, 2002]), it is $\overline{K}_d(z)$ that can be evaluated. Therefore the focus in this study is the variation of $\overline{K}_d(z)$, not $K_d(z)$. Note that the value represented by symbol K_d in many literatures [*McClain et al.*, 1996; *Sathyendranath and Platt*, 1988] is actually $\overline{K}_d(z)$ not the $K_d(z)$ defined by equation (1). Further, the symbol K_d used in this text generally refers to the concept of diffuse attenuation coefficient for E_d; its exact value can be either $K_d(z)$ or $\overline{K}_d(z)$.

[5] To get $\overline{K}_d$ value from ocean color remote sensing, one standard method uses empirical spectral ratios [*Austin and Petzold*, 1981; *Mueller and Trees*, 1997], another uses pigment concentrations ([C]) [*Morel*, 1988] with [C] also empirically derived from spectral ratios [*Gordon and Morel*, 1983; *O'Reilly et al.*, 1998]. Owing to the empirical approaches used in the algorithms, the derived $\overline{K}_d$ from both methods may contain big uncertainties [*Darecki and Stramski*, 2004]. *Mobley* [1994, p. 135] contends that the values of $\overline{K}_d$ at 450 nm estimated using [C] values can differ by a factor of 2 even for averaged case 1 waters [*Morel*, 1988]. A 30% error in $\overline{K}_d$ can result in a factor of 2 error in the calculated $E_d(E_{10\%})$ where $E_d(z)$ is 10% of $E_d(0)$. Therefore a factor of 2 error in $\overline{K}_d$ will lead to significantly wrong $E_d(E_{10\%})$ value.

[6] To understand the nature of K_d variations, efforts have been made to link K_d with water's inherent optical properties (IOPs) [*Preisendorfer*, 1976], such as absorption (a), scattering (b), and/or backscattering (b_b) coefficients. For instance, through Monte Carlo simulations, *Gordon* [1989] empirically approximated $K_d(0)$ as $1.04(a + b_b)/\mu_0$, with μ_0 the average cosine of the downwelling light just beneath the surface. *Kirk* [1984, 1991] and *Morel and Loisel* [1998] empirically modeled K_d of the euphotic zone ($\langle K_d \rangle$) as a function of a and b with the formula

$$\frac{\langle K_d \rangle}{a} = \frac{1}{\mu_0}\left(1 + G(\mu_0)\frac{b}{a}\right)^{0.5}. \tag{3}$$

$G(\mu_0)$ is a model parameter that determines the relative contribution of scattering to $\langle K_d \rangle$. Values of $G(\mu_0)$ are found to vary with both μ_0 and the volume scattering function (VSF) of the water medium [*Kirk*, 1991; *Morel and Loisel*, 1998]. For K_d of the upper half of the euphotic zone or K_d of the asymptotic value, they are also empirically expressed functions of a and b in earlier studies [*Gordon*, 1989; *Gordon et al.*, 1975; *Zaneveld*, 1989].

[7] VSF (or scattering phase function of particles) is a property that is seldom measured in the field and cannot be analytically derived from ocean color remote sensing. *Gordon* [1993] has found that below-surface upwelling radiance is not sensitive to change of b for a given b_b. Therefore values of b can hardly be accurately derived from ocean color remote sensing, because only signals of upwelling radiance are collected by a remote sensor. These limitations undermine the application of models

like equation (3) to estimate $\langle K_d \rangle$ (especially for ocean color remote sensing).

[8] On the other hand, it has been demonstrated that absorption (a) and backscattering (b_b) coefficients can be well retrieved from ocean color remote sensing [*Garver and Siegel*, 1997; *Hoge and Lyon*, 1996; *Lee et al.*, 2002, 1996; *Loisel and Stramski*, 2000; *Roesler and Boss*, 2003; *Roesler and Perry*, 1995]. The accuracy for a and b_b derived from remote-sensing reflectance can be within ~15% [*Hoge and Lyon*, 1996; *Lee et al.*, 2002; *Loisel and Stramski*, 2000; *Loisel et al.*, 2001], in contrast to the factor of 2 error in derived [*C*] [*Gordon and Morel*, 1983; *O'Reilly et al.*, 1998]. Therefore a more accurate approach is to evaluate $\overline{K}_d$ based on values of a and b_b (especially for remote sensing). For this strategy, $\overline{K}_d$ is often simplified as [*Smith and Baker*, 1981]

$$\overline{K}_d = a + b_b \tag{4a}$$

or [*Sathyendranath and Platt*, 1988; *Sathyendranath et al.*, 1989]

$$\overline{K}_d = (a + b_b)/\mu_0. \tag{4b}$$

These approximations, however, were not elaborated from radiative transfer. To establish a theoretical basis and to improve the determination of $\overline{K}_d$ using values of a and b_b, it is necessary to refine these simple approximations based on the radiative transfer equation (RTE).

3. General Form to Model $\overline{K}_d(z)$

[9] After integrating the RTE for the upward and downward light field, there is [*Aas*, 1987; *Stavn and Weidemann*, 1989]

$$\frac{dE_d(z)}{dz} = -\frac{a}{\mu_d(z)}E_d(z) - \frac{r_d(z)\,b_b}{\mu_d(z)}E_d(z) + \frac{r_u(z)\,b_b}{\mu_u(z)}E_u(z). \tag{5}$$

Here μ_d (μ_u) is the average cosine and r_d (r_u) are the shape factors for downwelling (upwelling) light field [*Stavn and Weidemann*, 1989], respectively. E_u is the upwelling irradiance. Apply the definition of R (ratio of E_u to E_d [*Gordon et al.*, 1980]) and the definition of $K_d(z)$ (equation (1)), there is

$$K_d(z) = \frac{1}{\mu_d(z)}\; a + \left(\frac{r_d(z)}{\mu_d(z)} - \frac{r_u(z)\,R(z)}{\mu_u(z)}\right)\; b_b. \tag{6}$$

As $\overline{K}_d(z)$ is the average of K_d between 0 m and z, $\overline{K}_d(z)$ can be expressed as

$$\overline{K}_d(z) = m_0(z)a + \mathrm{v}(z)\; b_b. \tag{7}$$

[10] Equation (7) is simply a rewrite of equation (6) by introducing two parameters (m_0 and v) to represent the combined effects of μ_d (μ_u) and r_d (r_u). This RTE-based expression reveals an important concept that has often been overlooked: theoretically the rates of contributions from a and b_b to $\overline{K}_d(z)$ (or $K_d(z)$) are not the same, i.e., $m_0 \neq v$, as opposed to the simplifications of equation (4). Further, when the distribution of the light field changes, m_0 and v may change accordingly.

[11] Since our objective is to obtain an a&b_b-based $\overline{K}_d(z)$ model that can be easily used for ocean color studies, the individual variations of μ_d (μ_u) or r_d (r_u) are not interested in here. Some analyses and discussions regarding those parameters can be found in the work of *Kirk* [1981], *Stavn and Weidemann* [1989], and *Ackleson et al.* [1994]. Our objective is the values and variations of m_0 and v. When m_0 and v are known, it is straightforward to calculate $\overline{K}_d(z)$ with known values of a and b_b. The values and variations of m_0 and v, however, are not directly derivable from the RTE or equation (6). As in earlier studies in developing semianalytical models for other apparent optical properties [*Lee et al.*, 2004; *Morel and Loisel*, 1998], the values and variations of m_0 and v are derived and analyzed from numerical simulations of the RTE.

4. Hydrolight Simulations

[12] As many studies [*Berwald et al.*, 1995; *Lee et al.*, 1998; *Mobley et al.*, 1993, 2002; *Morel and Loisel*, 1998], we used the widely accepted Hydrolight [*Mobley*, 1995] to simulate the subsurface light field. Values of $\overline{K}_d(z)$ were then calculated from the simulated $E_d(z)$ by equation (2).

[13] For Hydrolight simulations, the input data are solar light and water's IOPs. As those earlier studies, the downwelling irradiance at sea surface from the Sun and sky is simulated by the spectral model of *Gregg and Carder* [1990]. A wind speed of 5 m/s is assigned, and a series of water depths are selected. The required IOPs are the absorption and scattering coefficients and the particle phase function (PPF). As earlier studies [*Gordon*, 1989; *Kirk*, 1991; *Morel and Loisel*, 1998], these IOPs are kept vertically constant. Also, the scattering is separated into molecular and nonmolecular (collectively called particle) scatterings [*Gordon and Morel*, 1983; *Morel and Gentili*, 1993; *Sathyendranath et al.*, 2001]. The total absorption (a) and backscattering (b_b) coefficients are taken from the data set adopted by the International Ocean-Color Coordinating Group (see http://www.ioccg.org/groups/OCAG_data.html), which has 500 different spectra (400–800 nm with a step of every 10 nm) of a and b_b that cover wide dynamic ranges. Three realistic but significantly different PPFs are employed to provide different values of b for each b_b. One of the PPFs is the averaged particle phase function (AVGP) from Petzold's measurements [*Mobley et al.*, 2002; *Petzold*, 1972], which has a backscattering to total-scattering ratio ($\sigma = b_b/b$) of 1.83%. The other two PPFs are simulated by the Fournier-Fornad model [*Fournier and Forand*, 1994; *Mobley et al.*, 2002], with σ values as 1.0% (represented as FF010) and 4.0% (represented as FF040), respectively. Therefore for each b_b value, there are three significantly different b values in the numerical simulations.

[14] To reduce the calculation time but without losing representation of the dynamic range of the data set, a and b_b spectra were selected from the first data point with a step of 5. Therefore 100 pairs of a and b_b spectra (a(440) ranged from 0.016 to 3.1 m^{-1} and b_b(440) ranged from

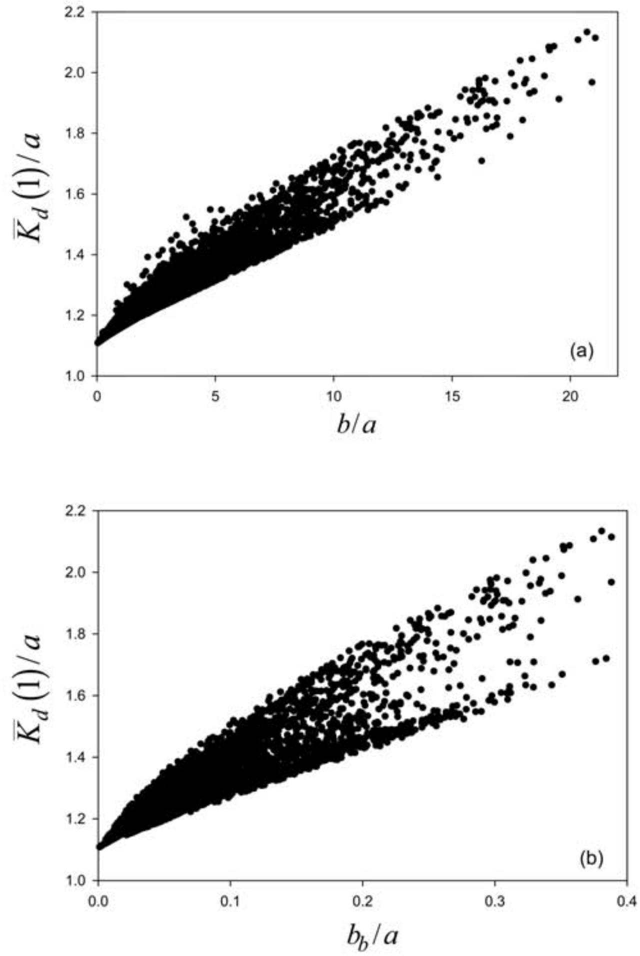

Figure 1. Hydrolight-simulated $\overline{K}_d(1)/a$ versus inherent optical properties (IOPs) (4100 points), with the Sun at 30° from zenith and particles following the averaged particle phase function (AVGP). (a) $\overline{K}_d(1)/a$ versus b/a. (b) $\overline{K}_d(1)/a$ versus b_b/a.

0.0034 to 0.113 m^{-1}) are used as IOP inputs for the Hydrolight simulations.

5. Results

5.1. Some Characteristics $\overline{K}_d(z)$

[15] As an example to show the variation of $\overline{K}_d(z)$, values of the diffuse attenuation coefficient between 0 m and 1 m ($\overline{K}_d(1)$, AVGP as PPF) are presented here, since similar results are found for other $\overline{K}_d(z)$. For data shown in Figure 1, the Sun is at 30° from zenith. Following *Kirk* [1984], Figure 1a plots the values of $\overline{K}_d(1)/a$ against the values of b/a, with Figure 1b showing $\overline{K}_d(1)/a$ against the values of b_b/a. Not surprisingly, as those shown by *Kirk* [1984] and *Morel and Loisel* [1998], $\overline{K}_d(1)/a$ increases with b/a due to increased scattering. $\overline{K}_d(1)/a$ spans a range of 1.1 to 2.2 for the different combinations of IOPs, and scatters about ±12% around its average value for a corresponding b/a (or b_b/a) value. The deviations of these $\overline{K}_d(1)/a$ values are wider compared to the $K_d(E_{10\%})/a$ shown by *Kirk* [1984]. This is because $K_d(E_{10\%})$ is a local value and is corresponding to a fixed ratio (10%) of $E_d(z)/E_d(0)$. The results in Figure 1a, however, are for fixed depth range (0–1 m) and have $E_d(1)/E_d(0)$ ranging from 98 to 0.2% due to the wide variations of IOPs. Since the light field at 1 m is different for the different IOPs, and K_d is a property depending on the distribution of light field, we see $\overline{K}_d(1)/a$ not a constant for the same b/a or b_b/a.

[16] To see how $\overline{K}_d$ (1) varies with a and b_b, Figure 2a shows the variation of $\overline{K}_d(1)/a$ versus b_b/a for a series of a values, while Figure 2b shows the variation of $\overline{K}_d(1)/a$ versus a for different b_b/a values. Apparently, for data shown in Figure 2a (total absorption coefficients varied from 0.03 to 1.0 m^{-1}), $\overline{K}_d(1)/a$ follow linear relationships with b_b/a (correlation coefficient (r^2) > 0.99). On the other hand, for the different b_b/a values (Figure 2b), $\overline{K}_d(1)/a$ increases with a, but in a nonlinear fashion and apparently approaching an asymptotic value. This phenomenon is consistent with the asymptotic theory [*McCormick*, 1992; *Zaneveld*, 1989] that eventually $K_d(z)$ approaches an asymptotic value at larger optical depths. Here the range of geometric depth is fixed between 0 and 1 m, but the increase of a and b_b will increase the optical depths.

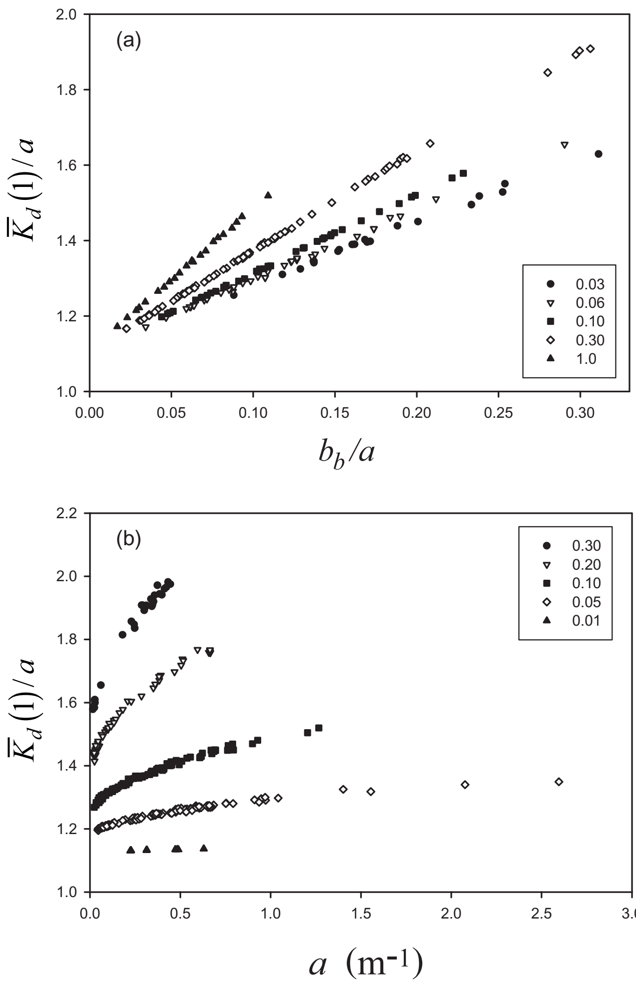

Figure 2. $\overline{K}_d(1)/a$ (a) versus b_b/a for different a values (in the box) and (b) versus a for different b_b/a values (in the box). All data are from Figure 1.

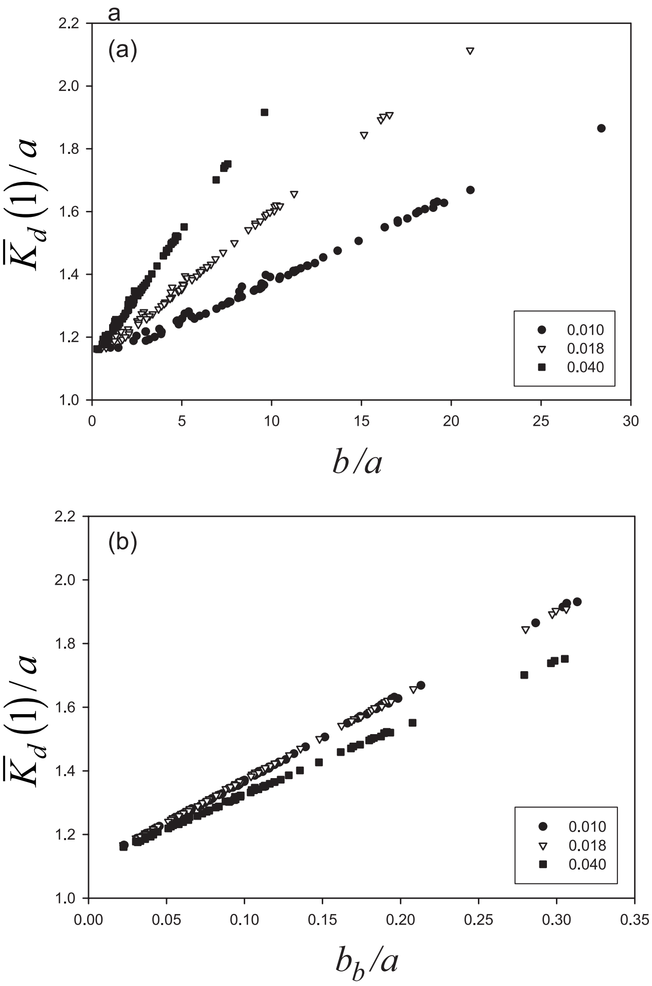

Figure 3. Hydrolight-simulated $\overline{K}_d(1)/a$ versus IOPs for particle phase functions with different b_b/b (in the box). The absorption coefficient is 0.3 m^{-1}, and the Sun is at 30° from zenith. (a) $\overline{K}_d(1)/a$ versus b/a. (b) $\overline{K}_d(1)/a$ versus b_b/a.

[17] For data shown in Figure 2a, the intercepts from linear regression analysis between $\overline{K}_d(1)/a$ and b_b/a are about the same (~1.12) for all absorption coefficients. The slope (value of v), however, differs a lot for various absorption coefficients. The v values range from 1.67 for a = 0.03 m^{-1} to 3.79 for a = 1.0 m^{-1}. These results indicate that (1) for different light fields (resulted from different a and b_b values), the contribution rate (value of v) of b_b to $\overline{K}_d(1)$ differs, as indicated by equation (7) and (2) the contribution rate of b_b to $\overline{K}_d(1)$ can be three times the rate of a to $\overline{K}_d(1)$. These results indicate that the simple $\overline{K}_d$ model (equations (4a) or (4b)) underestimates the contributions of b_b to $\overline{K}_d$. For particle free waters, *Gordon* [1989] found that the Sun angle-normalized $\overline{K}_d$ is about a + 1.44b_b. Apparently our results are consistent with that of *Gordon* [1989] for low-absorption waters. Note that the absorption coefficients of clearest natural water in the work of *Smith and Baker* [1981] were derived from $\overline{K}_d$ using equation (4a), and their values in the blue wavelengths are found to be larger than those measured by *Pope and Fry* [1997]. The actual dependence of $\overline{K}_d$ on a and b_b suggests that at least a portion of the difference can be removed if a more accurate $\overline{K}_d$ model is used in the derivation [*Gordon*, 1989].

5.2. $\overline{K}_d(1)$ for Different Particle Phase Functions

[18] The above only shows the variation of $\overline{K}_d(1)/a$ for one PPF; it is desired and important to know how $\overline{K}_d(1)/a$ varies with different particle phase functions (PPFs). As described earlier, Hydrolight simulations with three different PPFs were carried out. In these simulations, it was the same set of absorption and backscattering coefficients used. Change of PPF only changes the total scattering coefficient for each b_b. For example, Figure 3a shows $\overline{K}_d(1)/a$ versus b/a for the three different PPFs with the absorption coefficient set at 0.3 m^{-1}. Clearly, as shown by *Kirk* [1991] and *Morel and Loisel* [1998], $K_d(E_{10\%})$, $\langle K_d \rangle$, and $\overline{K}_d(1)$ vary significantly for different PPFs even a and b/a values are kept the same. These results further emphasis that knowing a and b is not enough for the estimation of K_d, and it is critical to know the PPF (or VSF) of the water in order to get accurate K_d when using models like equation (3).

[19] Figure 3b shows the relationship between $\overline{K}_d(1)/a$ and b_b/a for the data used in Figure 3a. Apparently, among the three realistic PPFs, the dependence of $\overline{K}_d(1)/a$ on b_b/a is much more stable than that of $\overline{K}_d(1)/a$ on b/a, though it is not clear why no apparent difference exists between the results using AVGP as PPF and that using FF010 as PPF. For the three PPFs with σ (= b_b/b) values varied by a factor of 4 (1.0% to 4.0%), the $\overline{K}_d(1)/a$ values deviate ±5% around its average for a b_b/a value. These results suggest that the contribution rates of a and b_b to $\overline{K}_d(1)$ for given a and b_b do not vary much for different b values. This is consistent with equation (7), and demonstrates that it is the absorption and backscattering coefficients contributing most to K_d. The forward scattering coefficient has only secondary effects on K_d. This result indicated that if a&b_b (along with other auxiliary information, such as solar altitude) are known, $\overline{K}_d(z)$ can be adequately calculated without exact knowledge of the particle phase function, as indicated in earlier studies [*Sathyendranath and Platt*, 1988; *Smith and Baker*, 1981]. This is important for ocean color remote sensing, as it can best provide the absorption and backscattering coefficients, not the PPF or VSF or b [*Gordon*, 1993].

5.3. Model $\overline{K}_d(z)$ as a Function of a&b_b

[20] To make the $\overline{K}_d(z)$ model (equation (7)) useful for ocean studies, how values of m_0 and v vary with water properties and solar zenith angle needs to be known. Figure 2a indicates that for a specified Sun angle m_0 is nearly a constant (~1.12), whereas v changes in a bigger range (1.67 to 3.79, for instance). Further, since data shown in Figure 2b suggests that v increases nonlinearly with a and reaches an asymptotic value for large a, slope v (which is also the contribution rate of b_b to K_d) is empirically modeled as follows:

$$v = m_1(1 - m_2 e^{-m_3 a}). \tag{8}$$

Combining equation (7) with equation (8), there is

$$\overline{K}_d(1) = m_0 a + m_1(1 - m_2 e^{-m_3 a}) b_b. \tag{9}$$

In this semianalytical relationship between $\overline{K}_d(1)$ and a&b_b, four model parameters (m_0, m_1, m_2, and m_3) are employed to

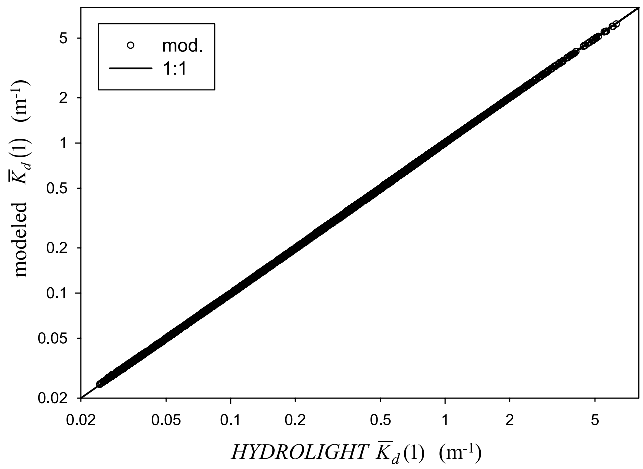

Figure 4. For data in Figure 1, $\overline{K}_d(1)$ from Hydrolight simulations versus $\overline{K}_d(1)$ modeled by equation (9).

explicitly quantify the contribution rates of a and b_b to $\overline{K}_d(1)$. Following the method described in many earlier studies [*Gordon*, 1989; *Kirk*, 1991; *Morel and Loisel*, 1998], the values of these model parameters (provided in Table 2) are derived by curve fitting all data points shown in Figure 1b with equation (9). Figure 4 compares the $\overline{K}_d(1)$ values modeled by equation (9) versus those calculated from Hydrolight simulations. As expected, excellent model results were obtained for these $\overline{K}_d(1)$ values, which span a range of three orders of magnitude (0.025–6.1 m^{-1}). The average error is less than 1% for all 4100 points, with a maximum error about 2%. Note that the model parameters are the same for all a&b_b, thus the $\overline{K}_d(1)$ model is independent of the biogeochemical-to-optical relationships, as long as values of a and b_b are provided.

[21] The above results show $\overline{K}_d(1)$ with the Sun at 30°. For studies in physical and biological oceanography [*Sathyendranath and Platt*, 1988] and for measurements made at a series of fixed depths (MOBY or HyCODE mooring [*Chang and Dickey*, 2004], for instance), it is desired to have a system that provides $\overline{K}_d(z)$ for other depths and Sun angles. On the basis of the results of $\overline{K}_d(1)$, a generalized model for $\overline{K}_d(z)$ is expressed as

$$\overline{K}_d(z,\theta_a) = m_0(z,\theta_a)\,a + m_1(z,\theta_a)\left(1 - m_2(z,\theta_a)\,e^{-m_3(z,\theta_a)a}\right) b_b. \tag{10}$$

In this model, the values of the four model parameters (m_0, m_1, m_2, m_3) are needed for desired solar altitude and depth. This requirement is fulfilled by a look-up table (LUT) [*Liu et al.*, 2002; *Morel and Gentili*, 1993]. For a few depths and solar altitudes, the derived model parameters (m_0, m_1, m_2, m_3) are provided in Table 2. Owing to the change of light distribution, values of m_0, m_1, m_2, and m_3 vary more or less with depth and solar altitude. Note that these values were derived with data satisfying $E_d(z)/E_d(0) > 10^{-5}$, simply because the $E_d(z)$ values that below 10^{-5} of $E_d(0)$ cannot be well measured in the field and make a negligible contribution to photosynthesis. For these $\overline{K}_d(z)$ data, the average error is ∼3% (maximum error ∼10%) between equation (10) modeled $\overline{K}_d(z)$ and Hydrolight determined $\overline{K}_d(z)$. For example, with the AVGP as PPF for particle scattering, Figure 5 shows modeled $\overline{K}_d(5)$ versus Hydrolight $\overline{K}_d(5)$ for the Sun at 10° and 60° from zenith, respectively.

5.4. K_d for the Euphotic Zone ($\overline{K}_d(E_{10\%})$)

[22] To simplify the process of calculating $E_d(z)$ of the surface layer and accept coarser approximations in calculated $E_d(z)$ [*Sathyendranath and Platt*, 1988], $\overline{K}_d(z)$ in the euphotic zone might be replaced by the value of $\overline{K}_d(E_{10\%})$, the K_d value between $E_d(0)$ and 10% of $E_d(0)$. Practically, this is the layer that contributes most to the photosynthesis of the water column [*Antoine et al.*, 1995; *Platt*, 1986]. Also, most signals measured by a remote sensor are originated in this surface layer [*Gordon and Mcluney*, 1975], and many field-measured K_d are derived from measurements made in this layer. As with the above model of $\overline{K}_d(z)$, values of m_0, m_1, m_2, and m_3 are derived for $\overline{K}_d(E_{10\%})$ from Hydrolight simulations and are provided (last row of Table 2). To include a wider range of $\overline{K}_d(E_{10\%})$ needed for better derivation of the (m_0, m_1, m_2, m_3) values, the $\overline{K}_d(E_{10\%})$ values from Hydrolight simulations were actually for $E_d(z)/E_d(0)$ between 8% and 12%, instead of the exact 10%. For these $\overline{K}_d(E_{10\%})$ values, the average error is ∼2% (maximum error ∼9%) between modeled and Hydrolight $\overline{K}_d(E_{10\%})$. As an example, Figure 6 presents modeled $\overline{K}_d(E_{10\%})$ versus Hydrolight $\overline{K}_d(E_{10\%})$ for the Sun at 30°. The data gap for $\overline{K}_d(E_{10\%})$ around 0.08 m^{-1} is due to the depth selection in the Hydrolight simulations resulting in no $\overline{K}_d(E_{10\%})$ around 0.08 m^{-1}. This data gap, however, has no impact on the application of the model as the agreement between modeled and known $\overline{K}_d(E_{10\%})$ is good for $\overline{K}_d(E_{10\%})$ in the range of ∼0.05–5.7 m^{-1}.

[23] Further, we found that for the four parameters the variations of m_1, m_2, and m_3 are limited for different solar altitude, while most variations happened in m_0 (see last row of Table 2). The variation of m_0 is conceptually consistent with the results shown by *Kirk* [1984] and *Gordon* [1989]. Since there is not much variation for m_1, m_2, and m_3, a set of

Table 2. Model Parameters for a Few Solar Altitudes and Depth Ranges

	m_0; m_1; m_2; m_3		
Range	10°	30°	60°
0–1 m	1.060; 4.307; 0.675; 1.484	1.118; 4.373; 0.657; 1.489	1.311; 4.461; 0.587; 2.980
0–5 m	1.048; 5.573; 0.727; 2.628	1.118; 5.462; 0.695; 2.631	1.312; 4.033; 0.447; 4.739
0–10 m	1.094; 4.148; 0.685; 6.854	1.146; 3.758; 0.664; 10.645	1.316; 3.506; 0.392; 11.966
0–20 m	1.049; 4.877; 0.786; 11.009	1.110; 4.615; 0.759; 12.404	1.267; 4.172; 0.488; 12.825
$\overline{K}_d(E_{10\%})$	1.044; 4.173; 0.530; 11.157	1.108; 4.245; 0.526; 10.942	1.320; 4.120; 0.504; 10.304

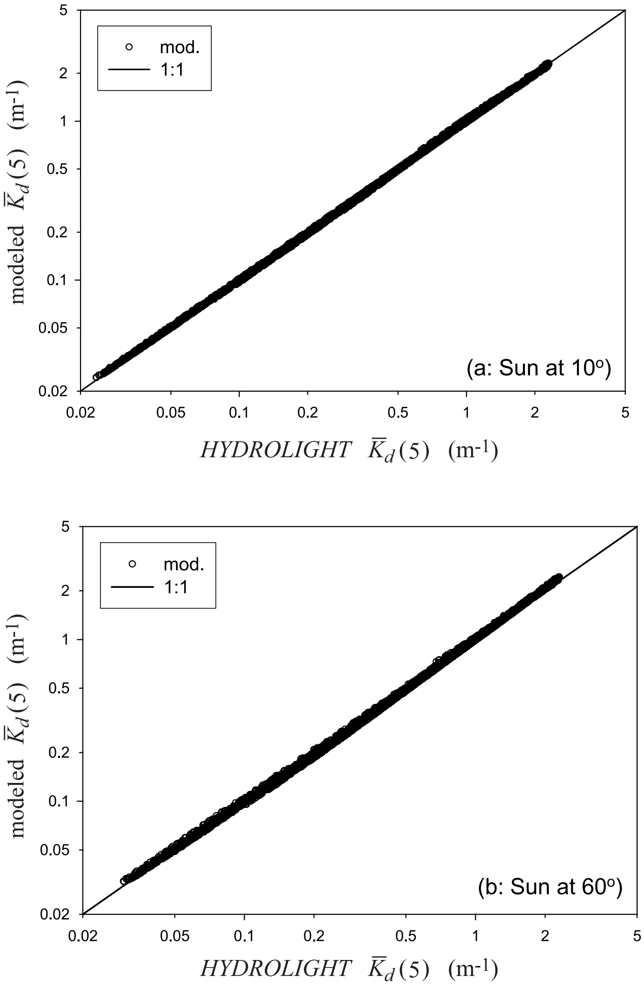

Figure 5. Modeled $\overline{K}_d(5)$ versus Hydrolight $\overline{K}_d(5)$ for the Sun at (a) 10° and (b) 60° from zenith.

averages for these parameters can be derived without losing much accuracy to modeled $\overline{K}_d(E_{10\%})$. For the variation of m_0 with solar altitude, extra Hydrolight simulations with the Sun at 20°, 40°, and 50° were carried out for the same IOPs. On the basis of all Hydrolight simulations, it is found that a generalized model for $\overline{K}_d(E_{10\%})$ can be

$$\overline{K}_d(E_{10\%}) = (1 + 0.005\theta_a)\, a + 4.18\left(1 - 0.52\, e^{-10.8\, a}\right) b_b. \quad (11)$$

Here θ_0 is the above surface solar zenith angle in degrees, such as 30 for instance. To simplify equation (11) to a concise form similar as those in earlier studies [*Gordon*, 1989; *Sathyendranath and Platt*, 1988] but with potentially larger errors followed, there is

$$\overline{K}_d(E_{10\%}) = (1 + 0.005\theta_a)\, a + 3.47\; b_b. \quad (12)$$

With equation (11) or equation (12), values of $\overline{K}_d(E_{10\%})$ can then be quickly determined when values of θ_a, a, and b_b are given.

5.5. Test the $\overline{K}_d(E_{10\%})$ Model With Data Simulated by Other PPFs

[24] The above presented results of $\overline{K}_d(E_{10\%})$ for one particle phase function. It is equally or more important to know the performance of this model to $\overline{K}_d(E_{10\%})$ values resulted from other phase functions. For this need, the above $\overline{K}_d(E_{10\%}) \Leftrightarrow a\&b_b$ model (equation (11)) is applied to the Hydrolight data simulated with the other two PPFs without any change in model parameters. Figure 7a shows the $\overline{K}_d(E_{10\%})$ comparison for FF010 and Figure 7b for FF040, where all data have the Sun at 60° from zenith. The average error is 2.1% (maximum error is 8.8%) for FF010, while the average error is 1.7% (maximum error is 11.7%) for FF040. Clearly, the model performed very well to both data sets. These kinds of results indicate that $\overline{K}_d(E_{10\%})$ values determined by equation (11) are reliable, though the PPF differed significantly (resulting in a factor of 4 difference in b values for each b_b). Like the results of $\overline{K}_d(1)$, the change of forward-scattering coefficients only showed insignificant effects on $\overline{K}_d(E_{10\%})$.

6. Discussion

[25] For studies of heat transfer and photosynthesis in the ocean, it requires to know the scalar irradiance at depth ($E_0(z)$) [*Morel*, 1978]. Fundamentally, $E_0(z)$ can be expressed as

$$E_0(z) = \frac{E_d(z)}{\mu_d(z)} + \frac{E_u(z)}{\mu_u(z)} = \left(\frac{1}{\mu_d(z)} + \frac{R(z)}{\mu_u(z)}\right) E_d(0) e^{-\overline{K}_d(z) z}. \quad (13)$$

In equation (13), $\mu_d(z)$ is generally in a range of 0.7–0.96 and $\mu_u(z)$ in a range (0.4–0.5) for all depths [*Berwald et al.*, 1995; *Kirk*, 1981; *Mobley*, 1994, p. 552], and R is generally less than 0.1 [*Kirk*, 1991; *Morel and Maritorena*, 2001; *Morel and Prieur*, 1977]. Thus it is clear that errors in E_0 at any depth resulted from uncertainties in $\mu_d(z)$ and $\mu_u(z)$ are quite limited. The critical parameter in the determination of E_0 at depth is $\overline{K}_d(z)$ (see equation (13)). For instance, a 30% error in $\overline{K}_d(z)$ can result in a factor of 2 error in $E_0(E_{10\%})$. Thus it is essential to get

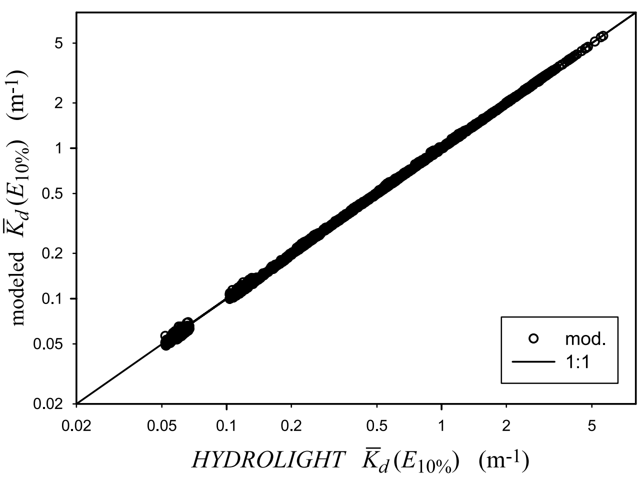

Figure 6. Modeled $\overline{K}_d(E_{10\%})$ versus Hydrolight $\overline{K}_d(E_{10\%})$ for the Sun at 30° from zenith.

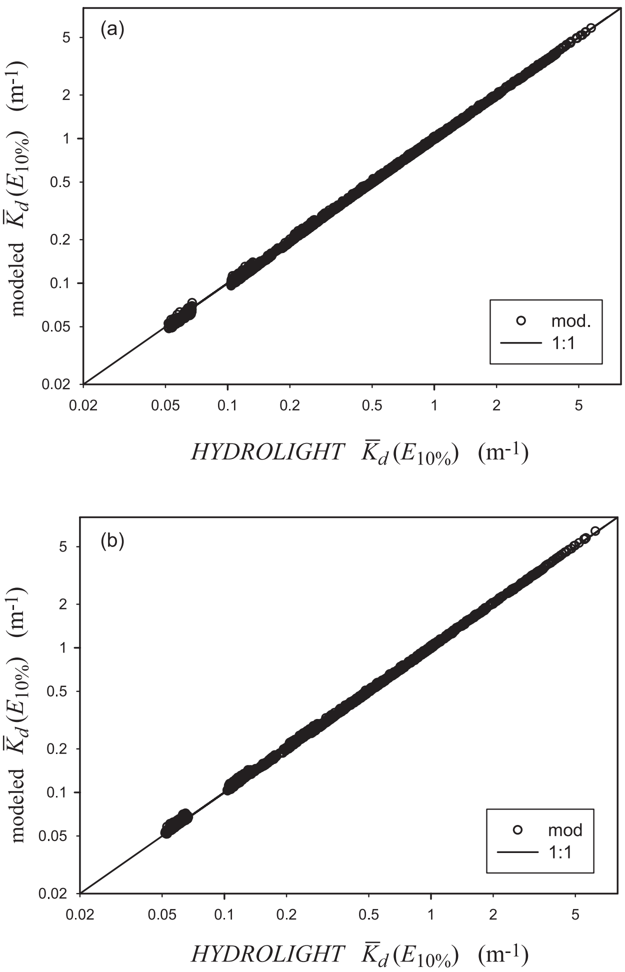

Figure 7. Comparison of $\overline{K}_d(E_{10\%})$ from Hydrolight simulations versus $\overline{K}_d(E_{10\%})$ determined by equation (11), a model developed using data with AVGP as particle phase function (PPF). (a) For Hydrolight data with FF010 as PPF. (b) For Hydrolight data with FF040 as PPF (see text for details).

accurate values of $\overline{K}_d(z)$, though better estimations of $\mu_d(z)$ and $\mu_u(z)$ will improve the evaluation of $E_0(z)$. Apparently a model like equation (10) or equation (11) for the diffuse attenuation coefficient of $E_0(z)$ can also be developed. This is omitted here in order to keep this study focused, also because (1) historically and currently values of $\overline{K}_d(z)$ are extensively measured in the field and (2) E_0 at depth can be well determined by equation (13) if the two important parameters ($E_d(0)$ and $\overline{K}_d(z)$) are known. For higher precision of $E_0(z)$ estimation, models regarding the variation of $\mu_d(z)$ and $\mu_u(z)$ [*Liu et al.*, 2002; *McCormick*, 1995; *Zaneveld*, 1989] could be adopted.

[26] At this point, a semianalytical model for the diffuse attenuation coefficient ($\overline{K}_d(z)$) is developed for vertically homogeneous and optically deep water. It is noticed that this semianalytically determined $\overline{K}_d(z)$ will not be as accurate as that determined from Hydrolight given the same IOPs and boundary conditions, but the explicit algebraic expression developed here processes data almost instantaneously for given IOPs, depths, and solar altitudes. This effectiveness is important for analyzing data from the vast ocean. Further, this model for $\overline{K}_d(z)$ along with the model for remote-sensing reflectance (R_{rs}) composes an explicit system for modeling and processing ocean color data. In this system (schematically depicted in Figure 8), there are three different links to relate the environmental properties, IOPs, and AOPs. Link I relates biogeochemical properties with IOP; Link II relates IOP with R_{rs} or irradiance reflectance (R); and Link III relates IOP with K_d. Links II and III are bridged by optical-to-optical properties, their models in general have fewer uncertainties when applied to a wide range of waters. Most of the uncertainties occur at Link I, where the conversion factors (e.g., pigment-specific absorption coefficient [*Bricaud et al.*, 1995; *Sathyendranath et al.*, 1987] or biogeochemical-specific scattering coefficient [*Gordon and Morel*, 1983; *Loisel and Morel*, 1998]) involved in the biogeochemical-to-optical relationships vary significantly over different regions and/or seasons, therefore regional/temporal relationships have to be adopted to cope with such variations. This is the link that needs increased efforts for the development of regional/temporal algorithms for the concentrations of those biogeochemical constituents.

[27] Since $a\&b_b$ are at the center of the modeling/processing system, and methods/algorithms have been developed to retrieve $a\&b_b$ from R_{rs} [*Carder et al.*, 1999; *Hoge and Lyon*, 1996; *Lee et al.*, 2002; *Loisel and Stramski*, 2000; *Roesler and Perry*, 1995], estimation of $\overline{K}_d(z)$ from remote sensing can now be carried out in a semianalytical fashion (Link III) that is independent of the derivation of the concentrations (such as [C]). Such an approach then avoids the large uncertainties associated with the [C] estimation [*O'Reilly et al.*, 1998], and provides a potential to signifi-

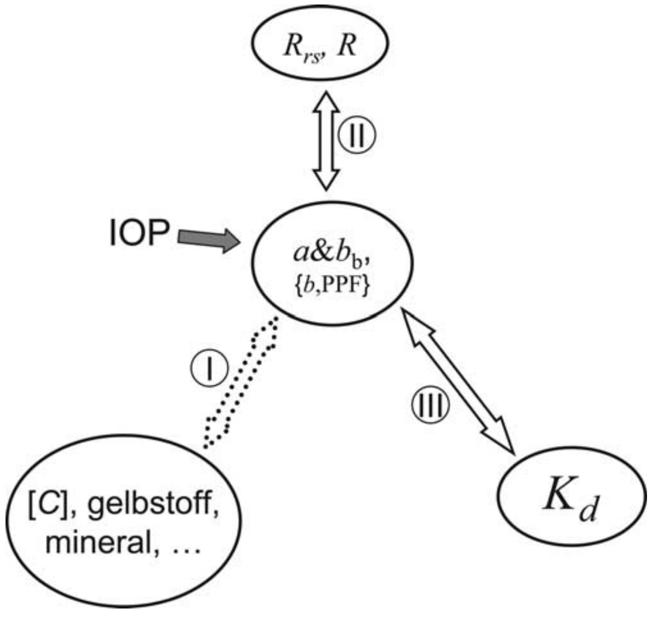

Figure 8. Structural relationships among biogeochemical concentrations, IOPs, R_{rs} (and/or R), and K_d.

cantly improve the determination of $\overline{K}_d(z)$ from ocean color remote sensing.

7. Conclusions

[28] On the basis of the radiative transfer equation and Hydrolight numerical simulations, a semianalytical model is developed for the diffuse attenuation coefficient of downwelling irradiance ($\overline{K}_d(z)$). As in some earlier studies [*Sathyendranath and Platt*, 1988; *Smith and Baker*, 1981], the model expresses $\overline{K}_d(z)$ as a function of absorption and backscattering coefficients, but it refined the earlier simple approximations so that the model is now consistent with the theory of radiative transfer and improves the determination of $\overline{K}_d(z)$. On the basis of extensive numerical simulations, the values of the model parameters are derived by fitting the data with the model. The model parameters vary with solar altitude and depth, but remain the same for different IOPs. At least for data used in this study, this $\overline{K}_d(z) \Leftrightarrow a\&b_b$ model can be used for data with realistic volume scattering function (or particle phase function). Since $a\&b_b$ can be well retrieved from ocean color remote sensing, the $\overline{K}_d(z)$ model developed here provides a route to quickly and semianalytically determine its values for pixels of the ocean. Also, for downwelling irradiances that are measured at a few fixed depths (such as MOBY, or TSRB of Satalantic, Inc., etc.), the model developed here provides a basis for the derivation of $a\&b_b$ from measured $\overline{K}_d(z)$.

[29] Compared to the $\overline{K}_d(z)$ from exact numerical simulations such as Hydrolight, there are a few percent of errors remaining in the semianalytically modeled $\overline{K}_d(z)$. Such types of errors are common in semianalytical approaches [*Gordon*, 1989; *Kirk*, 1991; *Sathyendranath and Platt*, 1997]. A semianalytical model, however, provides (1) an explicit way to easily understand the fundamental relationships between IOPs and AOPs [*Gordon et al.*, 1975; *Kirk*, 1991]; (2) a tool to instantaneously evaluate AOPs for given IOPs; and (3) a basis to quickly invert IOPs from AOPs [*Hoge and Lyon*, 1996; *Lee et al.*, 2002; *Loisel and Stramski*, 2000]. At present, calculation efficiency is important for studies of the vast ocean, and a few percent of error is much better than acceptable limits in remote sensing and uncertainties in field measurements. Therefore semianalytical models practically meet both efficiency and accuracy requirements needed for oceanographic studies.

[30] The values of the model parameters are derived with Hydrolight simulations under clear sky conditions and a wind speed of 5 m/s. Adjustments of those values are expected for cloudy conditions and high wind speed. Also, it is necessary to point out that the model developed here and the models of earlier studies [*Gordon*, 1989; *Gordon et al.*, 1975; *Kirk*, 1991; *Morel and Loisel*, 1998] are for vertically homogeneous waters, which are generally applicable for the surface mixed layer of the ocean [*Mueller and Lange*, 1989]. However, challenges remain to extend the models to vertically stratified waters, especially to remote sensing of the ocean where the extent of stratification of the surface layer is unknown when a satellite sensor makes measurements.

[31] **Acknowledgments.** Support for this study was provided by the Naval Research Laboratory's basic research P.E. 06010115N "Hyperspectral Characterization of the Coastal Zone" (NRL) and NASA grant NAG-W10288 (NRL). The authors are very grateful to C. D. Mobley for providing Hydrolight code and assistance and are in debt to Heather Melton Penta for editorial contribution of the manuscript. Comments and suggestions from two reviewers are greatly appreciated.

References

Aas, E. (1987), Two stream irradiance model for deep waters, *Appl. Opt.*, *26*, 2095–2101.
Ackleson, S. G., W. M. Balch, and P. M. Holligan (1994), Response of water-leaving radiance to particulate calcite and chlorophyll a concentrations: A model for Gulf of Maine coccolithophore blooms, *J. Geophys. Res.*, *99*, 7483–7499.
Antoine, D., A. Morel, and J.-M. André (1995), Algal pigment distribution and primary production in the eastern Mediterranean as derived from coastal zone color scanner observations, *J. Geophys. Res.*, *100*, 16,193–16,209.
Austin, R. W., and T. J. Petzold (1981), The determination of the diffuse attenuation coefficient of sea water using the coastal zone color scanner, in *Oceanography From Space*, edited by J. F. R. Gower, pp. 239–256, Springer, New York.
Berwald, J., D. Stramski, C. D. Mobley, and D. A. Kiefer (1995), Influences of absorption and scattering on vertical changes in the average cosine of the underwater light field, *Limnol. Oceanogr.*, *40*, 1347–1357.
Bricaud, A., M. Babin, A. Morel, and H. Claustre (1995), Variability in the chlorophyll-specific absorption coefficients of natural phytoplankton: Analysis and parameterization, *J. Geophys. Res.*, *100*, 13,321–13,332.
Carder, K. L., F. R. Chen, Z. P. Lee, S. K. Hawes, and D. Kamykowski (1999), Semianalytic Moderate-Resolution Imaging Spectrometer algorithms for chlorophyll a and absorption with bio-optical domains based on nitrate-depletion temperatures, *J. Geophys. Res.*, *104*, 5403–5421.
Chang, G. C., and T. D. Dickey (2004), Coastal ocean optical influences on solar transmission and radiant heating rate, *J. Geophys. Res.*, *109*, C01020, doi:10.1029/2003JC001821.
Clark, D. K., M. E. Feinholz, M. A. Yarbrough, B. C. Johnson, S. W. Brown, Y. S. Kim, and R. A. Barnes (2002), An overview of the radiometric calibration of MOBY, *Earth Observ. Syst.*, *6*, 64–67.
Darecki, M., and D. Stramski (2004), An evaluation of MODIS and SeaWiFS bio-optical algorithms in the Baltic Sea, *Remote Sens. Environ.*, *89*, 326–350.
Fournier, G. R., and J. L. Forand (1994), Analytic phase function for ocean water, *Proc. SPIE Soc. Opt. Eng.*, *12*, 194–201.
Garver, S. A., and D. A. Siegel (1997), Inherent optical property inversion of ocean color spectra and its biogeochemical interpretation: 1. Time series from the Sargasso Sea, *J. Geophys. Res.*, *102*, 18,607–18,625.
Gordon, H. R. (1989), Can the Lambert-Beer law be applied to the diffuse attenuation coefficient of ocean water?, *Limnol. Oceanogr.*, *34*, 1389–1409.
Gordon, H. R. (1993), Sensitivity of radiative transfer to small-angle scattering in the ocean: Quantitative assessment, *Appl. Opt.*, *32*, 7505–7511.
Gordon, H. R., and W. R. Mcluney (1975), Estimation of the depth of sunlight penetration in the sea for remote sensing, *Appl. Opt.*, *14*, 413–416.
Gordon, H. R., and A. Morel (1983), *Remote Assessment of Ocean Color for Interpretation of Satellite Visible Imagery: A Review*, 44 pp., Springer, New York.
Gordon, H. R., O. B. Brown, and M. M. Jacobs (1975), Computed relationship between the inherent and apparent optical properties of a flat homogeneous ocean, *Appl. Opt.*, *14*, 417–427.
Gordon, H. R., R. C. Smith, and J. R. V. Zaneveld (1980), Introduction to ocean optics, *Proc. SPIE Soc. Opt. Eng.*, *6*, 1–43.
Gregg, W. W., and K. L. Carder (1990), A simple spectral solar irradiance model for cloudless maritime atmospheres, *Limnol. Oceanogr.*, *35*, 1657–1675.
Hoge, F. E., and P. E. Lyon (1996), Satellite retrieval of inherent optical properties by linear matrix inversion of oceanic radiance models: An analysis of model and radiance measurement errors, *J. Geophys. Res.*, *101*, 16,631–16,648.
Jerlov, N. G. (1976), *Marine Optics*, Elsevier, New York.
Kirk, J. T. O. (1981), A Monte Carlo study of the nature of the underwater light field in, and the relationships between optical properties of, turbid yellow waters, *Aust. J. Mar. Freshw. Res.*, *32*, 517–532.

Kirk, J. T. O. (1984), Dependence of relationship between inherent and apparent optical properties of water on solar altitude, *Limnol. Oceanogr.*, *29*, 350–356.
Kirk, J. T. O. (1991), Volume scattering function, average cosines, and the underwater light field, *Limnol. Oceanogr.*, *36*, 455–467.
Lee, Z. P., K. L. Carder, T. G. Peacock, C. O. Davis, and J. L. Mueller (1996), Method to derive ocean absorption coefficients from remote-sensing reflectance, *Appl. Opt.*, *35*, 453–462.
Lee, Z. P., K. L. Carder, C. D. Mobley, R. G. Steward, and J. S. Patch (1998), Hyperspectral remote sensing for shallow waters: 1. A semianalytical model, *Appl. Opt.*, *37*, 6329–6338.
Lee, Z. P., K. L. Carder, and R. Arnone (2002), Deriving inherent optical properties from water color: A multi-band quasi-analytical algorithm for optically deep waters, *Appl. Opt.*, *41*, 5755–5772.
Lee, Z. P., K. L. Carder, and K. P. Du (2004), Effects of molecular and particle scatterings on model parameters for remote-sensing reflectance, *Appl. Opt.*, *43*, 4957–4964.
Lewis, M. R., M. Carr, G. Feldman, W. Esaias, and C. McMclain (1990), Influence of penetrating solar radiation on the heat budget of the equatorial pacific ocean, *Nature*, *347*, 543–545.
Liu, C.-C., K. L. Carder, R. L. Miller, and J. E. Ivey (2002), Fast and accurate model of underwater scalar irradiance, *Appl. Opt.*, *41*, 4962–4974.
Loisel, H., and A. Morel (1998), Light scattering and chlorophyll concentration in case 1 waters: A reexamination, *Limnol. Oceanogr.*, *43*, 847–858.
Loisel, H., and D. Stramski (2000), Estimation of the inherent optical properties of natural waters from the irradiance attenuation coefficient and reflectance in the presence of Raman scattering, *Appl. Opt.*, *39*, 3001–3011.
Loisel, H., D. Stramski, B. G. Mitchell, F. Fell, V. Fournier-Sicre, B. Lemasle, and M. Babin (2001), Comparison of the ocean inherent optical properties obtained from measurements and inverse modeling, *Appl. Opt.*, *40*, 2384–2397.
Marra, J., C. Langdon, and C. A. Knudson (1995), Primary production, water column changes, and the demise of a Phaeocystis bloom at the Marine Light-Mixed Layers site (59°N, 21°W) in the northeast Atlantic Ocean, *J. Geophys. Res.*, *100*, 6633–6644.
McClain, C. R., K. Arrigo, K.-S. Tai, and D. Turk (1996), Observations and simulations of physical and biological processes at ocean weather station P, 1951–1980, *J. Geophys. Res.*, *101*, 3697–3713.
McCormick, N. J. (1992), Asymptotic optical attenuation, *Limnol. Oceanogr.*, *37*, 1570–1578.
McCormick, N. J. (1995), Mathematical models for the mean cosine of irradiance and the diffuse attenuation coefficient, *Limnol. Oceanogr.*, *40*, 1013–1018.
McCormick, N. J., and N. K. Hojerslev (1994), Ocean optics attenuation coefficients: Local versus spatially averaged, *Appl. Opt.*, *33*, 7067–7069.
Mobley, C. D. (1994), *Light and Water: Radiative Transfer in Natural Waters*, Elsevier, New York.
Mobley, C. D. (1995), Hydrolight 3.0 users' guide, report, SRI Int., Menlo Park, Calif.
Mobley, C. D., B. Gentili, H. R. Gordon, Z. Jin, G. W. Kattawar, A. Morel, P. Reinersman, K. Stamnes, and R. H. Stavn (1993), Comparison of numerical models for computing underwater light fields, *Appl. Opt.*, *32*, 7484–7504.
Mobley, C. D., L. K. Sundman, and E. Boss (2002), Phase function effects on oceanic light fields, *Appl. Opt.*, *41*, 1035–1050.
Morel, A. (1978), Available, usable, and stored radiant energy in relation to marine photosynthesis, *Deep Sea Res.*, *25*, 673–688.
Morel, A. (1988), Optical modeling of the upper ocean in relation to its biogenous matter content (case 1 waters), *J. Geophys. Res.*, *93*, 10,749–10,768.
Morel, A., and D. Antoine (1994), Heating rate within the upper ocean in relation to its bio-optical state, *J. Phys. Oceanogr.*, *24*, 1652–1665.
Morel, A., and B. Gentili (1993), Diffuse reflectance of oceanic waters: 2. Bi-directional aspects, *Appl. Opt.*, *32*, 6864–6879.
Morel, A., and H. Loisel (1998), Apparent optical properties of oceanic water: Dependence on the molecular scattering contribution, *Appl. Opt.*, *37*, 4765–4776.
Morel, A., and S. Maritorena (2001), Bio-optical properties of oceanic waters: A reappraisal, *J. Geophys. Res.*, *106*, 7163–7180.
Morel, A., and L. Prieur (1977), Analysis of variations in ocean color, *Limnol. Oceanogr.*, *22*, 709–722.
Mueller, J. L. (2000), SeaWiFS algorithm for the diffuse attenuation coefficient, K (490), using water-leaving radiances at 490 and 555 nm, in *SeaWiFS Postlaunch Calibration and Validation Analyses*, part 3, edited by S. B. Hooker, pp. 24–27, NASA Goddard Space Flight Cent., Greenbelt, Md.
Mueller, J. L., and R. E. Lange (1989), Bio-optical provinces of the northeast Pacific Ocean: A provisional analysis, *Limnol. Oceanogr.*, *34*, 1572–1586.
Mueller, J. L., and C. C. Trees (1997), Revised SeaWiFS prelaunch algorithm for diffuse attenuation coefficient K(490), *NASA Tech. Memo.*, *TM-104566*, vol. 41, 18–21.
Ohlmann, J. C., D. Siegel, and C. Gautier (1996), Ocean mixed layer radiant heating and solar penetration: A global analysis, *J. Clim.*, *9*, 2265–2280.
O'Reilly, J., S. Maritorena, B. G. Mitchell, D. Siegel, K. L. Carder, S. Garver, M. Kahru, and C. McClain (1998), Ocean color chlorophyll algorithms for SeaWiFS, *J. Geophys. Res.*, *103*, 24,937–24,953.
Petzold, T. J. (1972), Volume scattering functions for selected natural waters, technical report, Scripps Inst. of Oceanogr., La Jolla, Calif.
Platt, T. (1986), Primary production of ocean water column as a function of surface light intensity: Algorithms for remote sensing, *Deep Sea Res.*, *33*, 149–163.
Platt, T., S. Sathyendranath, C. M. Caverhill, and M. Lewis (1988), Ocean primary production and available light: Further algorithms for remote sensing, *Deep Sea Res.*, *35*, 855–879.
Pope, R., and E. Fry (1997), Absorption spectrum (380–700 nm) of pure waters: II. Integrating cavity measurements, *Appl. Opt.*, *36*, 8710–8723.
Preisendorfer, R. W. (1976), *Hydrologic Optics*, vol. 1, *Introduction*, Natl. Tech. Inf. Serv., Springfield, Va.
Roesler, C. S., and E. Boss (2003), Spectral beam attenuation coefficient retrieved from ocean color inversion, *Geophys. Res. Lett.*, *30*(9), 1468, doi:10.1029/2002GL016185.
Roesler, C. S., and M. J. Perry (1995), In situ phytoplankton absorption, fluorescence emission, and particulate backscattering spectra determined from reflectance, *J. Geophys. Res.*, *100*, 13,279–13,294.
Sathyendranath, S., and T. Platt (1988), The spectral irradiance field at the surface and in the interior of the ocean: A model for applications in oceanography and remote sensing, *J. Geophys. Res.*, *93*, 9270–9280.
Sathyendranath, S., and T. Platt (1997), Analytic model of ocean color, *Appl. Opt.*, *36*, 2620–2629.
Sathyendranath, S., L. Lazzara, and L. Prieur (1987), Variations in the spectral values of specific absorption of phytoplankton, *Limnol. Oceanogr.*, *32*, 403–415.
Sathyendranath, S., T. Platt, C. M. Caverhill, R. E. Warnock, and M. R. Lewis (1989), Remote sensing of oceanic primary production: Computations using a spectral model, *Deep Sea Res.*, *36*, 431–453.
Sathyendranath, S., G. Cota, V. Stuart, M. Maass, and T. Platt (2001), Remote sensing of phytoplankton pigments: A comparison of empirical and theoretical approaches, *Int. J. Remote Sens.*, *22*, 249–273.
Simpson, J. J., and T. D. Dickey (1981), Alternative parameterizations of downward irradiance and their dynamic significance, *J. Phys. Oceanogr.*, *11*, 876–882.
Smith, R. C., and K. S. Baker (1981), Optical properties of the clearest natural waters, *Appl. Opt.*, *20*, 177–184.
Stavn, R. H., and A. D. Weidemann (1989), Shape factors, two-flow models, and the problem of irradiance inversion in estimating optical parameters, *Limnol. Oceanogr.*, *34*, 1426–1441.
Tyler, J. E. (1960), Radiance distribution as a function of depth in an underwater environment, *Bull. Scripps Inst. Oceanogr.*, *7*, 363–411.
Zaneveld, J. R. V. (1989), An asymptotic closure theory for irradiance in the sea and its inversion to obtain the inherent optical properties, *Limnol. Oceanogr.*, *34*, 1442–1452.
Zaneveld, J. R. V., J. C. Kitchen, and H. Pak (1981), The influence of optical water type on the heating rate of a constant depth mixed layer, *J. Geophys. Res.*, *86*, 6426–6428.

R. Arnone and Z.-P. Lee, Naval Research Laboratory, Code 7333, Stennis Space Center, MS 39529, USA. (arnone@nrlssc.navy.mil; zplee@nrlssc.navy.mil)

K.-P. Du, State Key Laboratory of Remote Sensing Science, Research Center for Remote Sensing and GIS, School of Geography, Beijing Normal University, 5 Yushan Road, Beijing 100875, China. (kpdu@bnu.edu.cn)